Cavity generation in dental enamel using a copper-HyBrID laser

W. Miyakawa · A. M. Pizzo · M. C. B. S. Salvadori ·
J. T. Watanuki · R. Riva · D. M. Zezell

Abstract Applications of Cu-HyBrID laser (copper laser with **Hy**drogen **Br**omide **I**n **D**ischarge) in Dentistry and AFM (atomic force microscopy) evaluations of dental tissues irradiated by laser are seldom reported in the literature. This work presents an AFM investigation of the cross-section of a cavity generated in human dental enamel by laser thermal evaporation using the Cu-HyBrID laser. The results exposed the structural and morphological differences between the fused and non-fused dental enamel, provide qualitative information about the susceptibility of these tissues to abrasive polishing, and revealed the extension of the thermal damage. Quantitative information concerning the wall thickness and the dimensions of the cross-section of non-fused enamel rod were also obtained.

W. Miyakawa (✉) · J. T. Watanuki · R. Riva
Department of Photonics, Instituto de Estudos Avançados –
Centro Técnico Aeroespacial, Rodovia dos Tamoios,
km 5,5, Sao Jose dos Campos, SP 12231-970, Brazil
e-mail: wmi@ieav.cta.br

A. M. Pizzo · M. C. B. S. Salvadori
Instituto de Física – Universidade de São Paulo, Sao Paulo,
SP, Brazil

D. M. Zezell
Instituto de Pesquisas Energéticas e Nucleares, Cidade
Universitãria, Av. Lineu Prestes 2242, Sao Paulo,
SP 05508-000, Brazil

Introduction

Depending on the purpose, different lasers have been used in Dentistry. Despite the low absorption by dental hard tissues, even visible lasers have met applications in areas like caries prevention [1, 2], laser curing of sealants [3], caries diagnosis [4], etc.

Amongst the visible lasers, the Cu-HyBrID laser (copper laser with **Hy**drogen **Br**omide **I**n **D**ischarge [5, 6]) stands out as pulsed source of coherent radiation, emitting two wavelengths (510 nm and 578 nm), both of them with high output peak power (20 kW), short temporal pulse width (20–30 ns) and high repetition rates (5–20 kHz) [7]. However, applications of this laser in Dentistry are not frequently found in the literature.

Y. Yamada et al. [8] have tried to ablate human enamel and dentine with the green line (510 nm) of a copper vapor laser. According to these authors, experiments were performed using 2 W of mean output power, 3.3 kHz of pulse repetition rate, 0.6 cm^2 of beam spot size and one second of exposure time. Ablation was achieved only if dental tissues were covered by a thin layer of a photoabsorber (red or black ink).

Evaluation of the cross-section of cavities generated in dental tissues by lasers traditionally used in Dentistry (Nd:YAG, Er:YAG and CO_2 lasers) has also been subject of current interest. M. K. Yamada et al. [9] just reported the characteristics of these cavities, observed by a three-dimensional analyzer installed in a scanning electron microscope.

The atomic force microscopy (AFM), on its turn, has been used to evaluate several aspects of human dental enamel: the surface demineralization/remineralization

[10, 11], the ultrastructure alterations due to hypoplasia [12], and the mechanical properties on nanometer scale [13]. Even the surface of the adsorbed layer of salivary pellicle formed in vivo on dental enamel has been examined [14], but laser irradiated dental surfaces evaluations by AFM [15, 16] are rarely reported in the literature.

Hence, the purpose of this paper is to present an AFM investigation of the cross-section of a cavity generated by thermal evaporation in human dental enamel (without photoabsorber) using the 510 nm line of a Cu-HyBrID laser.

Materials and methods

An enamel block was cut from the most plane face of the crown of a non-erupted and freshly extracted human third molar. Before the cut, the tooth was only washed in distilled water and stored in 0.9% sodium chloride solution until the moment of use.

Figure 1 shows a schematic diagram of the experimental setup utilized to generate the cavities. The Cu-HyBrID laser used in this work was built at the Instituto de Estudos Avançados [7]. It emits radiation with high quality factor (M^2 = 4,9) [17], 20 kW of output peak power at 13–16 kHz of repetition rate, with pulse temporal width of 17 ns in the yellow line and 25 ns in the green line. An optical filter F was set in the laser beam pathway in order to reflect the yellow and transmit the green radiation. The lens f had 23 cm of focal length, and the values of the distances a (between the lens and the sample) and b (between the shutter and the sample) were 23 cm and 1 cm, respectively. This setup provided a 40 μm beam spot size over the sample surface. The electronic shutter c controlled the exposure time and it was adjusted to open during 40 ms and to repeat the cycle at each 0.5 s. Hence, working with an energy density of 20.7 J/cm^2 per pulse (1.0 GW/cm^2 of peak intensity) in the green line at
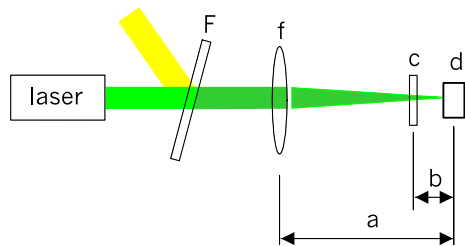

Fig. 1 Schematic diagram of the experimental setup where F is an optical filter, f is a focusing lens, c is an electronic shutter and d is the sample. Distances a and b are 23 cm and 1 cm, respectively

16 kHz of repetition rate, three random points of the enamel block were irradiated without any kind of photoabsorber. The first one received 10 shutter pulses, the second one, 15 and the third, 20 shutter pulses. Table 1 presents the corresponding number of laser pulses.

The irradiated enamel block had its surface previously evaluated by light microscopy. Next, it was embedded in acrylic resin and laterally polished (600-grit and 1200-grit sandpapers and 6 μm and 3 μm diamond paste) with the purpose of exposing the cross-section of the central portion of the cavity formed by laser. All this process was monitored with the light microscope until the desired cross-section was attained. As the polishing had overtaken the central position in the first trials, the procedure was twice restarted with the others cavities. The final polished surface corresponds to the third cavity cross-section. This surface was evaluated by atomic force microscopy using conventional Si_3N_4 tip in contact mode and J-scanner (Nanoscope IIIa, Digital Instruments).

Results

Figure 2 shows light microscopy images of the three points in the enamel block irradiated by the Cu-HyBrID laser. It can be clearly seen that the laser promoted thermal melting and evaporation of dental enamel, yielding cavities with approximately 185 μm diameter size. The walls of these cavities were formed by melted and re-solidified enamel and carbonization outlined all the edge of each cavity. Beyond this carbonization, there was apparently no other sign of thermal damage in the tissue surface.

Figure 3 presents a light micrograph of the final polished surface, exposing the desired cross-section of the third cavity and indicating the regions where the AFM analyses were performed. The numbered sites refer to: the region of the bottom of the cavity (1), which was fulfilled by acrylic resin, the region of the wall of the cavity (2), which is formed by melted and resolidified enamel and the region of non-fused enamel (3).

Table 1 Correlation between the number of shutter pulses and the number of laser pulses

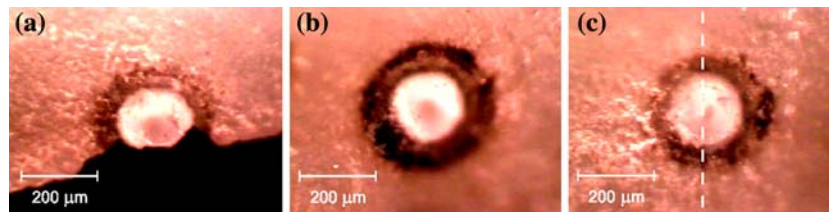| Number of shutter pulses	Number of laser pulses
10	6400
15	9600
20	12800

Fig. 2 Light microscopy images of the three points of the enamel surface that received 10 (**a**), 15 (**b**) and 20 (**c**) shutter shots. The dashed line in (**c**) corresponds to the desired cross-section of a central portion of the cavity that was evaluated by atomic force microscopy

The AFM images obtained on these regions are exhibited in Fig. 4. Images (a) and (b) correspond to region 1, images (c) and (d) correspond to region 2 and image (e), to region 3.

Figure 5 displays these five AFM images superposed, creating a single image with a larger field. Observe that cross-sections of non-fused enamel rods (in the upper right corner of the figure) are noticeably well delineated. According to the basic literature about the dental enamel [18, 19], these structures can be described as an arrangement of round prisms or cylindrical rods separated by inter-prismatic regions. These structures and arrangement of rods are strongly modified in the cavity walls (approximately in the diagonal of the figure), as they underwent melting and re-solidification in a different pattern. The assembled image also suggests that except for the two cracks, thermal alterations do not propagate beyond the walls of the cavity.

Figure 6 shows three-dimensional visualizations of non-fused enamel rods. In image (a), it is presented a 50 μm × 50 μm micrograph, where the scale in the x- and y-axis is 10 μm per division and it is expanded to 1 μm per division in the z-axis, emphasizing the sample
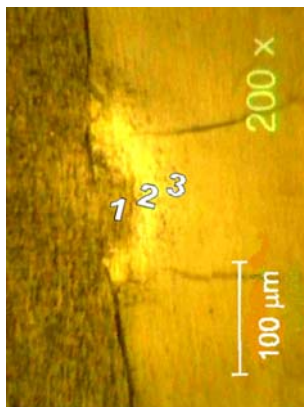

Fig. 3 Light micrograph of the final polished surface indicating the regions where the AFM analyses were performed

profile. In image (b), a 20 μm × 20 μm micrograph of same region, also expanded in the z-direction is shown. Finally, image (c) presents the section analysis of this region, giving an idea of the size of the enamel rod cross-section in this particular case (10.7 μm × 6.5 μm). According to the literature [18], the enamel rod cross-sections can vary in size and morphology throughout the enamel thickness and also depends on the angle between the sectioned plane and the rod long axis. Perfectly orthogonal planes in relation to the enamel rod long axis are not easily obtainable.

In Fig. 7, AFM section analyses referring to a vertical (a), a diagonal (b) and a horizontal (c) cross-section of the image (d) of Fig. 4 are available. According to image (b), the wall at the bottom of the cavity is 20 μm thick. In the profile curves (the upper left corner of Fig. 7 (a), (b) and (c)), it is interesting to note that the melted and re-solidified enamel region (between the two small triangles) is always in a higher level comparing with the non-fused enamel (at the right of the second triangle) and with the acrylic regions (at the left of the first triangle). On the other hand, the acrylic region is always in a lower level comparing with the other two regions. As the sample was polished, this fact indicates that the fused and re-solidified enamel is mechanically harder and less susceptible to abrasive polishing while, conversely, the acrylic region is softer and easily polished.

Discussions

Dental tissues are poor absorbers and strong scatterers of radiation with wavelength in the visible range of the electromagnetic spectrum. The absorption coefficient is typically small ($\mu_a \leq 1.0$ cm^{-1} at 510 nm for human dental enamel [20]), which means that the optical absorption length ($L = 1/\mu_a$) is large in comparison with better-absorbed wavelengths ($\mu_a \cong 1000$ cm^{-1} at 10.6 μm of a CO_2 laser for dental enamel [21]). Consequently, heat will not be generated only in a

Fig. 4 AFM evaluations of the cavity cross-section where images (**a**) and (**b**) correspond to region 1 in Figure 3; images (**c**) and (**d**) correspond to region 2 and (**e**), to region 3 in Figure 3
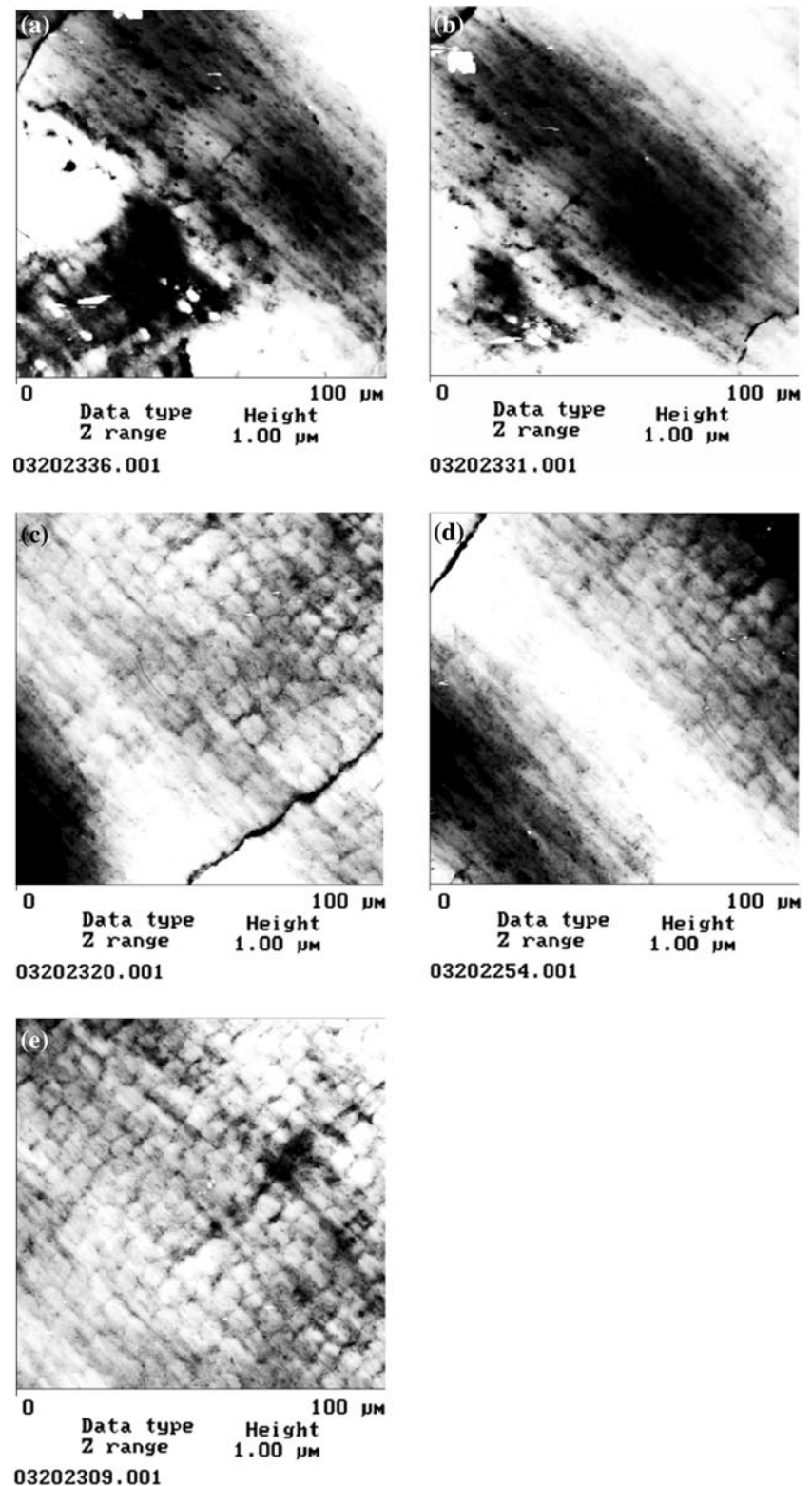
thin surface layer of the tissue but in a volumetric region considerably deeper [22]. Particularly for pulsed lasers like the Cu-HyBrID laser, the energy deposited by each laser pulse in the interaction volume and

consequently, the quantity of heat generated in this volume will be modest. A probable mechanism of laser-tissue interaction involves a volumetric cumulative process where each pulse causes a small temperature
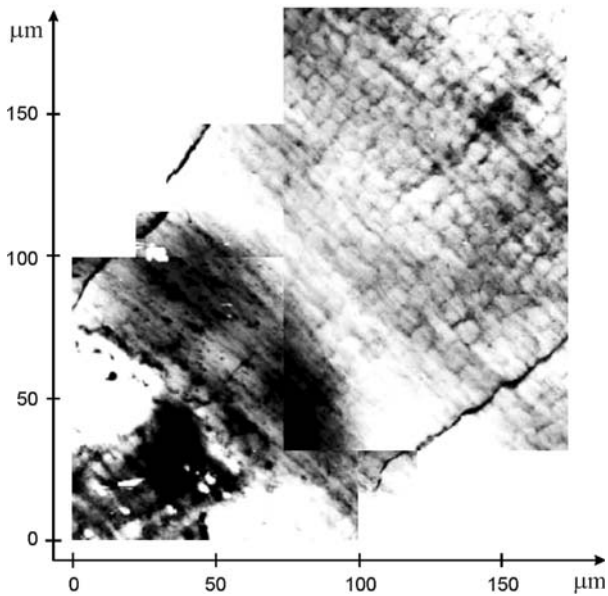
Fig. 5 Assembly with the five images of Figure 4, equivalent to a single image with a larger field of vision

rise. From the end of each pulse until the beginning of the next pulse, heat will diffuse throughout the dental tissue and temperature will decrease to a residual value. The net temperature increment after the pulse cycle (pulse duration + interpulse time) will then be given by the tissue temperature before the pulse cycle minus the residual temperature. Hence, depending on the laser parameters (pulse fluence, pulse repetition rate) and on the tissue thermal properties (specific heat, thermal diffusivity), the sample temperature will increase gradual and cumulatively. After a sufficiently great number of pulses, the melting temperature will be reached, leading to the formation of a melting pool. Again, depending on the thermal properties of the liquid phase, this melting pool may not re-solidify during the time between two successive pulses and the liquid removal will possibly occur by evaporation, either in the next pulse or in a new cumulative process. A numerical model based on the Monte Carlo method to calculate the temperature distribution on tooth after applying several laser pulses, whose wavelength is weakly absorbed and strongly scattered, is under development. It is expected that this numerical model helps the comprehension of the laser-tissue interaction, especially for low absorbing and highly scattering tissues, and gives support to the cumulative pulse mechanism for thermal melting and evaporation of human dental enamel by Cu-HyBrID laser radiation.

Y. Yamada et al. [8] probably did not attained their goal without the use photoabsorbers due to the combination of two factors: the low laser pulse fluence
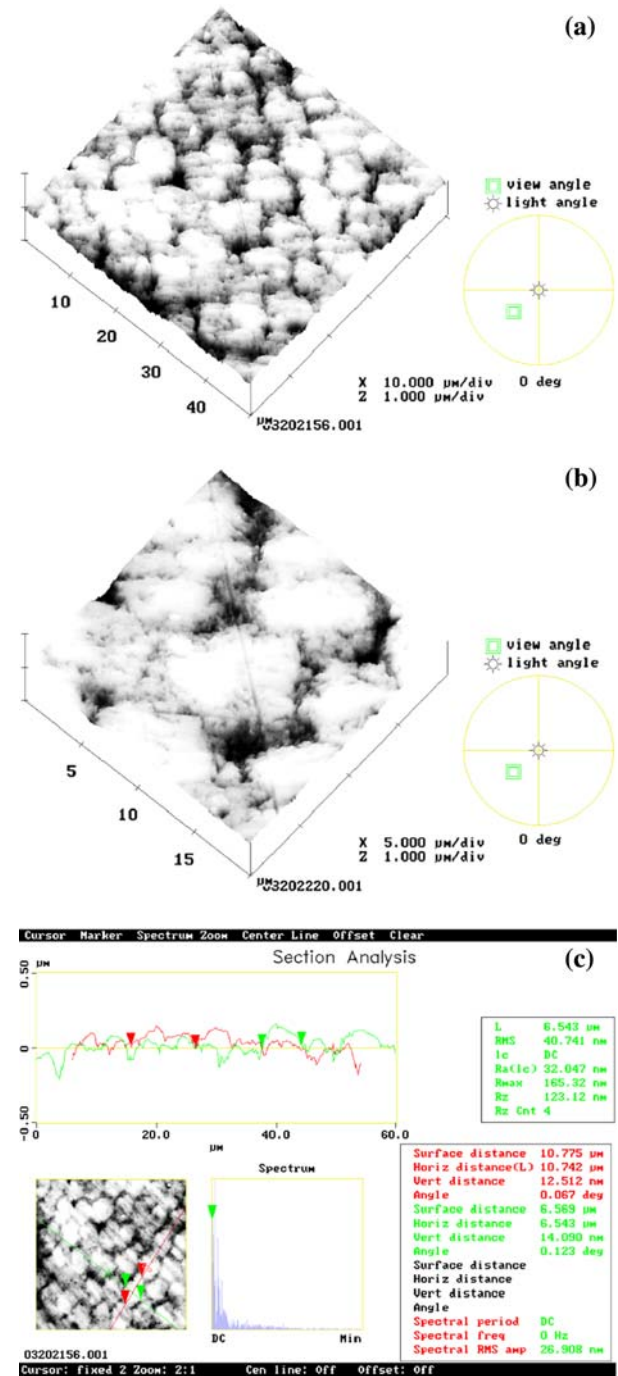

Fig. 6 3D images of non-fused dental enamel with (**a**) 50 μm × 50 μm and (**b**) 20 μm × 20 μm of scanning area. In image (**c**), section analysis was used to evaluate the dimensions of the enamel rod cross-sections (10.7 μm × 6.5 μm)

(~ 1.0 J cm^2), which generated an insufficient amount of heat per pulse and the relative long term between successive pulses (~ 300 μs), which allowed heat diffusion throughout the dental tissues before any considerable temperature increase and consequently, phase change occurrence.
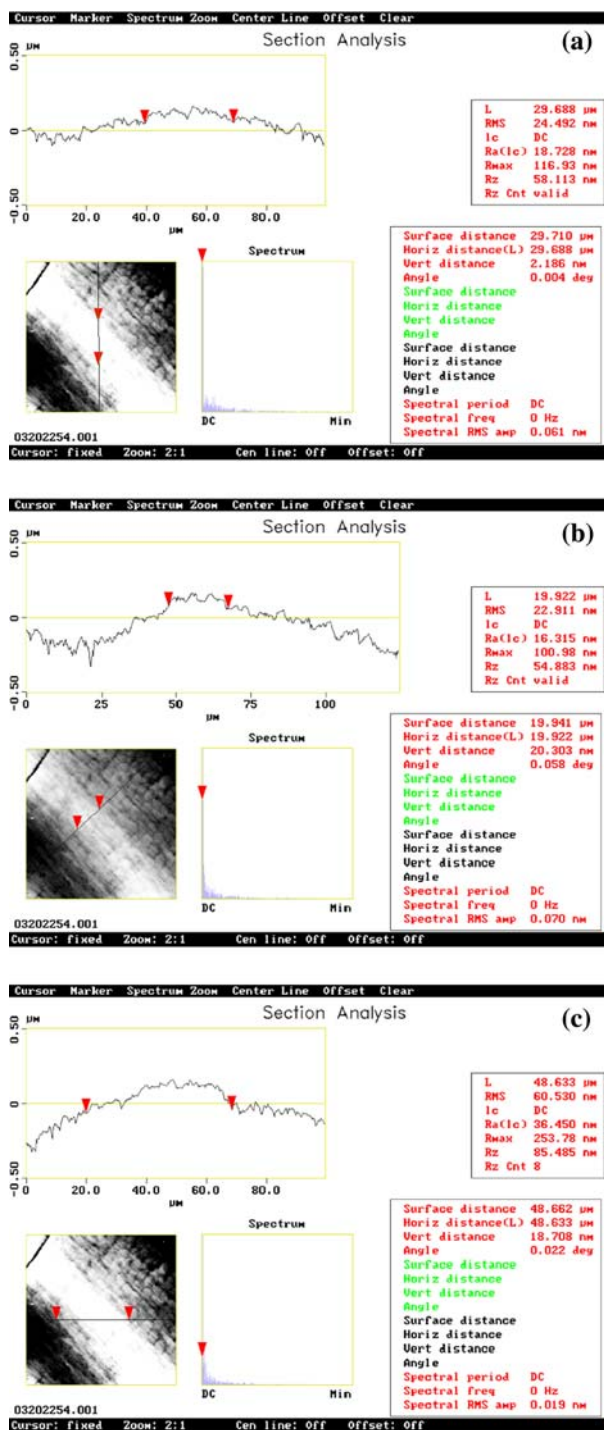
Fig. 7 AFM section analysis of image (**d**) of Figure 4

Direct comparison of the cavity cross-sectional profile generated by the Cu-HyBrID laser with the profiles reported by M. K. YAMADA [9] cannot be done because laser parameters and irradiation conditions are distinct. Roughly, the flat crater generated by the CO_2 laser reflects the high absorbability of the

10.6 μm wavelength by the dental enamel. The laser energy is deposited practically only in the enamel surface and the crater shape results from surface tissue melting and re-solidification. For Er:YAG laser, the cavity is deeper and the walls have an imbricate pattern. As the 2.94 μm wavelength is preferably absorbed by water ($\mu_a \cong 11850$ cm^{-1} [23]) and absorption by hydroxyapatite ($\mu_a \cong 640$ cm^{-1} [23]) is lower than for CO_2 laser, the optical absorption length is larger. Therefore, the volume of laser-tissue interaction is also deeper. By absorbing the laser energy, water is transformed in vapor, whose rapid expansion ruptures the enamel structure, leaving an imbricate aspect to the cavity walls. For Nd:YAG laser, the absorption coefficient of dental enamel at 1.06 μm ($\mu_a \cong 0.1$ cm^{-1} [24]) is as low as at 510 μm of the Cu-HyBrID laser. The surface morphologic alterations observed were probably induced by the heat generated by the carbon ink, which was applied in the enamel surface. If the ink was not used and appropriate laser parameters were employed, possibly the cavity cross-sectional profile would be similar to the profile obtained in this work: a deep cavity with melted and re-solidified walls.

Conclusions

AFM evaluation of the cross-section of a cavity generated by thermal evaporation in human dental enamel using the Cu-HyBrID laser was possible. The AFM was a good technique for exposing the structural and morphological differences between the fused and re-solidified enamel from the walls of the cavity and the non-fused enamel rods of the normal tissue. Except for the cracks, the images revealed that thermal damages do not propagate beyond the walls of the cavity. The wall at the bottom of the cavity is 20 μm thick and is less susceptible to abrasive polishing than the non-fused enamel region.

References

1. C. M. FLAITZ, M. J. HICKS, G. H. WESTERMAN, J. H. BERG, R. J. BLANKENAU and G. L. POWELL, *Pediatr. Dent.* **17** (1995) 31
2. R. J. BLANKENAU, G. L. POWEL, R. W. LELLIS and G. H. WESTERMAN, *J. Clin. Laser Med. & Surg.* **17** (1999) 241

3. C. M. FLAITZ, M. J. HICKS, R. J. BLANKENAU, G. H. WESTERMAN and G. L. POWELL, *Pediatr. Dent.* **13** (1991) 391

4. J. J. TEN BOSCH, in Proceedings. of the 1st Annual Indiana Conference, Indiana University, School of dentistry, 1996, edited by G. K. STOOKEY (1996) 81

5. E. S. LIVINGSTONE and A. MAITLAND, *J. Phys. E: Sci. Instrum.* **22** (1989) 63

6. E. S. LIVINGSTONE, D. R. JONES, A. MAITLAND and C. E. LITTLE, *Opt. Quantum Electron* **24** (1992) 73

7. R. RIVA, J. T. WATANUKI, N. A. S. RODRIGUES and C. SCHWAB, in Separation Phenomena in Liquids and Gases Fifth Workshop Proceedings, Foz do Iguaçu, Brazil, 1996, edited by C. SCHWAB, N. A. S. RODRIGUES and H. G. WOOD, (1996) 241

8. Y. YAMADA, Y. NAKAMURA, M. HOSSAIN, T. JOE, T. KAWANAKA and K. MATSUMOTO, *J. Clin. Med. & Surg.* **17** (1999) 249

9. M. K. YAMADA, M. UO, S. OHKAWA, T. AKASAKA and F. WATARI, *J. Biomed. Mater. Res. Part B: Appl. Biomater.* **71B** (2004) 7

10. F. LIPPERT, D. M. PARKER and K. D. JANDT, *J. Colloid and Interface Science* **280** (2004) 442

11. F. LIPPERT, D. M. PARKER and K. D. JANDT, *Surface Science* **553** (2004) 105

12. N. BATINA, V. RENUGOPATAKRISHNAN, P. N. C. LAVIN, J. C. H. GUERRERO, M. MORALES, R. GARDUNO-JUAREZ and S. L. LAKKA, *Calcif. Tissue Int.* **74** (2004) 294

13. S. HABELITZ, S. J. MARSHALL, G. W. MARSHALL and M. BALOOCH, *Arch. Oral Biol.* **46** (2001) 173

14. M. HANNIG, S. HERZOG, S. F. WILLIGEROTH and R. ZIMEHL, *Colloid and Polymer Science* **279** (2001) 479

15. F. WATARI, *J. Mat. Sci.: Mat. Med.* **12** (2001) 189

16. W. MIYAKAWA, A. M. PIZZO, M. C. B. S. SALVADO-RI, N. A. S. RODRIGUES and D. M. ZEZELL, *Acta Microscopica* **10**(Suppl. 1) (2001) 129

17. M. A. P. GIAO, W. MIYAKAWA, N. A. S. RODRIGUES, D. M. ZEZELL, R. RIVA, M. G. DESTRO, J. T. WATANUKI and C. SCHWAB, *Opt. Laser Technol.* **38** (2006) 523–527

18. D. R. EISENMANN, in "Oral Histology: Development, Structure, and Function", (4th ed.) edited by A. R. TEN CATE (1994) 239

19. O. FEJERSKOV and A. THYLSTRUP, in *"Histology of the human tooth"*, (2nd ed.) edited by I. A. MJÖR and O. FEJERSKOV, (1979) 75

20. D. FRIED, R. E. GLENA, J. D. B. FEATHERSTONE and W. SEKA, *Appl. Opt.* **34** (1995) 1278

21. D. YU, J. L. FOX, J. HSU, G. L. POWELL and W. I. HIGUCHI, *Opt. Eng.* **32** (1993) 298

22. J. F. LI, L. LI and F. H. STOTT, *Int. J. Heat Mass Transfer* **47** (2004) 1159

23. T. G. BARTON, H.-J. FOTH, M. CRHIST and K. HÖRMAN, *Appl. Opt.* **36** (1997) 32

24. W. SEKA, D. FRIED, J. D. B. FEATHERSTONE and S. F. BORZILLARY, *J. Dent. Res.* **74** (1995) 1086